Physica C 468 (2008) 2392–2398

Contents lists available at ScienceDirect

Physica C

journal homepage: www.elsevier.com/locate/physc

Phase purity and superconductivity of ruthenocuprates $Ru_ySr_2Gd_{1.5}Ce_{0.5}Cu_2O_{10-\delta}$

Y. Hata *, Y. Uragami, H. Yasuoka

Department of Applied Physics, National Defense Academy, 1-10-20 Hashirimizu, Yokosuka 239-8686, Japan

ARTICLE INFO

Article history:
Received 10 March 2008
Received in revised form 24 July 2008
Accepted 8 September 2008
Available online 16 September 2008

PACS:
74.25.Ha

Keywords:
Ru-1222
Magnetic superconductor
Weak ferromagnetism

ABSTRACT

$Ru_ySr_2Gd_{1.5}Ce_{0.5}Cu_2O_{10-\delta}$ ($y = 0.9$, 0.95, 1.0, 1.05 and 1.1) were synthesized by a solid-state reaction. The phase purity of the specimens was examined by X-ray powder diffraction and their superconductivity was confirmed by resistivity measurements. All the specimens exhibited superconductivity and contained small amounts of impurity phases of $SrRuO_3$, Sr_2RuGdO_3 and $RuSr_2GdCu_2O_8$. $Ru_{1.1}Sr_2Gd_{1.5}Ce_{0.5}Cu_2O_{10-\delta}$ contained the least amount of impurities and had the highest superconducting transition temperature. Two magnetic transitions were observed at 128 and 88.5 K in both the dc magnetization measurements and the ac susceptibility measurements. It is concluded that the former transition originates from the weak ferromagnetic transition of $RuSr_2GdCu_2O_8$ and the latter transition corresponds to the weak ferromagnetic transition of Ru ions in $Ru_{1.1}Sr_2Gd_{1.5}Ce_{0.5}Cu_2O_{10-\delta}$. The isothermal magnetization curve was derived from fundamental and higher-harmonic complex susceptibility measurements. The magnetization curve consists of a hysteresisless diamagnetism component and a component that is typical for magnetization of the mixed state in a type-II superconductor. The former is due to intragrain superconductivity and the latter is due to intergrain superconductivity. The intergrain critical current density at 5 K is estimated to be 0.75 A/cm^2 and it is several orders of magnitude lower than that of the ceramic $YBa_2Cu_3O_{7-\delta}$.

1. Introduction

The coexistence of superconductivity and long-range magnetic order such as ferromagnetism has been discussed for several decades [1,2]. Recently, the coexistence of the superconductivity and magnetism has been observed in ruthenocuprates $RuSr_2GdCu_2O_8$ (Ru-1212) and $RuSr_2RE_xCe_{2-x}Cu_2O_{10-\delta}$ (RERu-1222, RE = Gd, Sm and Eu). The magnetism in ruthenocuprates essentially originates from the RuO_2 sheets while superconductivity occurs in the CuO_2 layers. Recently, many reports have focused on the Ru-1212 phase in which the magnetic transition is observed at 133 K and superconductivity is observed below $T_c = 16$ K [3]. These experimental results are considered to be evidence for the coexistence of superconductivity and magnetism in Ru-1212. However, many important questions, including the details of the magnetic order and the mechanism that permits the coexistence of superconductivity and magnetism, have yet to be resolved. The study of μSR [3,4], neutron diffraction [5,6] and magneto-optics [9] confirmed the coexistence of magnetism and superconductivity in Ru-1212. On the other hand, some researchers have proposed the possibility of phase separation; that is, the separation of superconducting and magnetic regions [10,12,13]. The relation between superconductivity and the existence of an Ru vacancy, and the possibility of phase separation have been discussed by Kawashima et al. [14] and Petrykin et al. [13] for Ru-1212 and EuRu-1222, respectively.

Another issue that needs to be resolved for ruthenocuprates is the nature of the long-range magnetic order that coexists with superconductivity. In the case of Ru-1212, this point is complicated since magnetization measurements and NMR studies [11] suggest the existence of a ferromagnetic component and a neutron diffraction study [5] suggests the Ru moment has antiferromagnetic order. Consequently, it is widely accepted that the magnetism of Ru-1212 is weak ferromagnetism. It is considered that the ferromagnetic component of Ru-1212 originates from the canting of the Ru moment [7]. This canting is caused by rotation of the RuO_6 octahedra [8]. To date, no microscopic measurement of the magnetic state, such as neutron diffraction or NMR measurements, has been reported for RERu-1222. The magnetic properties of RERu-1222 are more complicated than those of Ru-1212. In particular, two magnetic transitions were found in magnetization measurements of RERu-1222 [15]. Felner et al. studied the magnetic properties of EuRu-1222 and $Ru_{1-x}Mo_xSr_2Eu_{1.5}Ce_{0.5}Cu_2O_{10}$ by conducting magnetization measurements and ^{57}Fe doped EuRu-1222 by ^{57}Fe Mössbauer spectroscopy. They suggested possible origins

* Corresponding author. Tel.: +81 46 841 3810; fax: +81 46 844 5912.
E-mail address: hata@nda.ac.jp (Y. Hata).

0921-4534/$ - see front matter © 2008 Elsevier B.V. All rights reserved.
doi:10.1016/j.physc.2008.09.006

of the two magnetic transitions: heterogeneity of the Ru valence and an impurity phase of scattered islands of the mixed Sr—Cu—Ru—O_3 phase.

This paper focuses on GdRu-1222. To clarify the natures of the superconductivity and magnetism of GdRu-1222, $Ru_ySr_2Gd_{1.5}Ce_{0.5}Cu_2O_{10-\delta}$ was synthesized. The phase purity of the sample was evaluated by Rietveld refinement of the X-ray powder diffraction pattern. Its magnetic properties were measured by dc magnetization measurements and ac susceptibility measurements to investigate the magnetism and the superconductivity of GdRu-1222.

2. Experiment

Polycrystalline samples of $Ru_ySr_2Gd_{1.5}Ce_{0.5}Cu_2O_{10-\delta}$ (y = 0.9, 0.95, 1.0, 1.05 and 1.1) were synthesized by the solid-state reaction of RuO_2, $SrCO_3$, Gd_2O_3 and CuO powders. The mixtures were first calcined in air at 850 °C for 12 h and 880 °C for 24 h. They were then ground, pressed into pellets and sintered in a flowing oxygen atmosphere at 1100 °C for 34 h with an intermediate grinding. The samples were annealed in a flowing oxygen atmosphere at 600 °C for 48 h.

The phase purity of the samples was characterized by powder X-ray diffraction. X-ray diffraction patterns were obtained by a MAC Science MXP3 diffractometer using Cu Kα radiation with a scanning step of $\delta 2\theta = 0.02^\circ$. The diffraction patterns were refined by Rietveld analysis using the RIETAN2000 program [16].

The temperature dependence of the resistivity was measured by the conventional four-probe method in a temperature range between room temperature and 4.2 K with a measurement current of 10 mA. The dc magnetization measurements were performed by a commercial SQUID magnetometer (Quantum Design, MPMS-5XL).

The fundamental and higher-harmonic complex susceptibilities $\chi_n = \chi'_n - i\chi''_n$ were measured by a susceptibility measurement system consisting of a Hartshorn bridge, a two-phase lock-in amplifier and two function generators. A function generator was used to apply an ac magnetic field $H_{ac}\cos(\omega t)$ to the samples. The amplitude of the ac magnetic field was $H_{ac} = 10$ mOe for the measurements of the temperature dependence of the susceptibilities, while an amplitude of $H_{ac} = 1$ Oe was used for the isothermal magnetization curve measurements. A second function generator was used as the reference for a lock-in amplifier to measure the higher-harmonic susceptibilities. The time-dependent magnetization $M(\omega t)$ of a specimen can be expressed in the form of a Fourier expansion,

$$M(\omega t) = \chi_0 H_{dc} + H_{ac}\sum_{n=1}^{\infty}[\chi'_n\cos(n\omega t) + \chi''_n\sin(n\omega t)], \quad (1)$$

where $\chi_0 H_{dc}$ is the dc offset due to geomagnetism and other sources. The Fourier coefficients of the cosine and sine series were defined as the real and imaginary parts of χ_n, respectively. The isothermal magnetization curve can be derived by substituting the measured values of χ'_n and χ''_n at a specified temperature into Eq. (1). With the exception of $n = 2$, the even harmonics of χ'_n and χ''_n and the harmonics for $n \geqslant 9$ were negligibly small and were neglected in this analysis.

3. Results and discussion

3.1. Sample characterization

Fig. 1 reveals that the main phase of all the samples is GdRu-1222 with a tetragonal 1222 type structure. The indexed peaks correspond to the peaks from GdRu-1222 and the asterisks indicate the peaks due to the impurities Sr_2GdRuO_6, $SrRuO_3$ and $RuSr_2GdCu_2O_8$. The peak intensities of the impurities Sr_2GdRuO_6 and $RuSr_2GdCu_2O_8$ decrease with increasing y, and the peak of $SrRuO_3$ is observed for the sample with $y = 1.1$.

The diffraction patterns were refined by Rietveld analysis to determine the mass fractions of GdRu-1222 and the impurities. The crystal structure model of GdRu-1222 reported by Knee et al. [17] was used. The crystal structure models of the impurity phases Sr_2GdRuO_6, $SrRuO_3$ and $RuSr_2GdCu_2O_8$ reported by Doi et al. [19], Kiyama et al. [18] and Chmaissem et al. [8], respectively, were used. The intensity data of the 2θ region between 10° and 90° were used for the analysis. The refined lattice parameters and the reliability factors, R_p and R_{wp}, are listed in Table 1. The mass fractions of GdRu-1222, $RuSr_2GdCu_2O_8$, Sr_2GdRuO_6 and $SrRuO_3$ are shown in Fig. 2 and Table 2. The mass fractions of Sr_2GdRuO_6 of $y = 1.1$ and $SrRuO_3$ of $y = 0.9$—1.05 were fixed at zero because they converged to a negative value. The mass fractions of $RuSr_2GdCu_2O_8$ and $SrGdRuO_6$ decrease with increasing y. The sample with $y = 1.1$ contains the least impurities of the synthesized samples.

The temperature dependence of the resistivity for GdRu-1222 is shown in Fig. 3. All samples exhibit superconductivity. As Table 1 shows, the sample with $y = 1.1$ has the highest T_c with a sharp

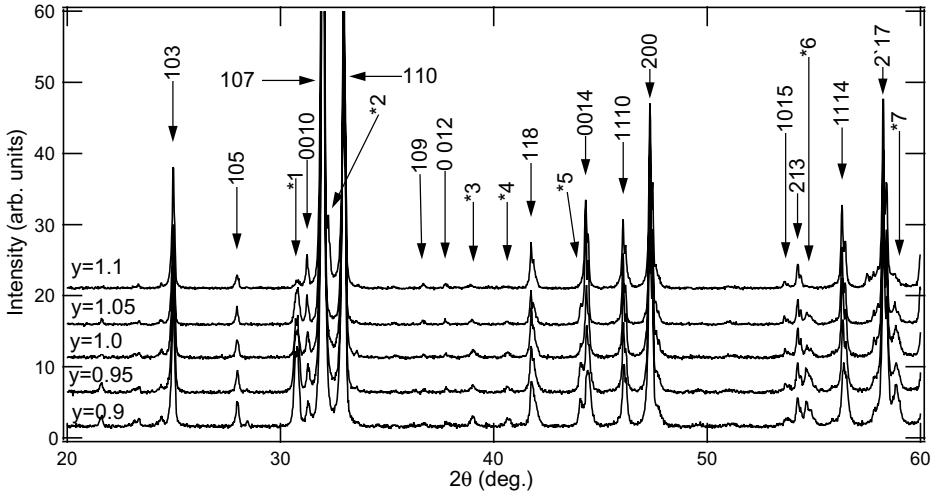

Fig. 1. Expanded view of X-ray diffraction patterns of $Ru_ySr_2Gd_{1.5}Ce_{0.5}Cu_2O_{10-\delta}$. The intensities are normalized for the peak intensities of 107 reflection to 100. The peaks from $Ru_ySr_2Gd_{1.5}Ce_{0.5}Cu_2O_{10-\delta}$ are indexed. The peaks denoted by an asterisk are impurity phases. (*1, *4, *5, *6: Ru_2SrGdO_6; *2: $SrRuO_3$; *3, *7: $RuSr_2GdCu_2O_8$).